16th Australasian Wind Engineering Society Workshop
Brisbane, Australia
18-19 July, 2013

A coupled parametric-CFD study for determining ages of downbursts

E. Abd-Elaal, J.E Mills and X. Ma

School of Natural and Built Environments

University of South Australia, Adelaide, South Australia 5001, Australia

Abstract

Downburst wind events cause great threats to many structural systems, especially large ones such as transmission line systems. The total age of downburst events are rarely investigated, however, it is an important parameter during the investigation of large extended structure systems. An established parametric study has been coupled with numerical CFD simulations to investigate observed downburst events. The different parameters of the downbursts such as the total age, intensity period, decay period, downburst diameter, initial location, path direction and parent storm translation speed, have all been estimated by relating the recorded field data to the coupled parametric-CFD study.

Introduction

The Australian severe storms archive of the last five years (February 2008 to February 2013) recorded more than 40 different accidental failures and damage events for transmission line systems due to severe wind, downbursts and tornadoes (Bureau of Meteorology, 2013). Owing to the importance of this type of wind load, many researchers have investigated downburst events. However, the total age of event and the intensity period of the events are still poorly defined. The importance of the decay and the period of the event arise during studies of large structures or systems. Shehata et al (2005) investigated the required number of spans for structural analysis of transmission line systems under microburst wind loads. They inspected transmission line systems with internal spans of 480.0 m and required at last 8 panels. However, the steady state simulation cannot provide accurate description for wind distribution on such extended spans, where the wind distribution continuously changes during the event age.

Wilson et al (1984) concluded from several recorded field events that downbursts reach their maximum horizontal speed during a time of 30 minutes from initial observation, 53% reach maximum before 5 minutes and 95% before 10 minutes. Hjelmfelt (1988) concluded that the downbursts increase in strength nearly linearly from first observation to maximum intensity, but then may quickly decay or exhibit a period of constant strength as shown in Figure 1. Chay (2006) and Abd-Elaal et al (2012) employed the observations of Hjelmfelt (1988) for developing an intensity decay function for an analytical model. They considered a period from 5 to 9 minutes for linear intensification, then 5 to 9 minutes for exponential decay (Figure 1).

The numerical and experimental simulations almost ignored the age of downbursts, they either neglected the downburst age completely or employed the suggested time function g(t) developed by Anderson et al (1992). However, there is a clear difference between the employed intensity-decay function in the analytical models and the one utilised in numerical models. In the same way, the observed temporal wind speed profiles by Hjelmfelt (1988) have different behaviours (Figure 1). The main question in the current research is obtaining the actual age for downburst event, that is required during studying or analysis several structural systems.

Factors affecting the recorded data

Several factors can change the recorded data significantly by increasing or decreasing the intensity and decay periods. One of the most significant factors is the parent storm translation speed, where the recorded field data at the stationary anemometer is a vector summation of downburst speed and parent storm speed. The storm translation speed increases the downburst velocity in the front of the storm and reduces the downburst speed in the rear. This can give wrong information about the decay and the intensity periods. However, the main problem is that this causes a rapidly changing location of downburst during the life cycle. For instance, if the translation speed is 15m/s then in a 3 minute period the centre of downburst will travel 2700 m or inversely, the location of observation will travel 2700 m for a stationary downburst which produces large effects on the observed data. In addition the recorded speed is a vector summation of translation speed and downburst speed, so the direction of the downburst path relative to the anemometer location point has another effect.

Other factors that can effect the recorded field data include the age of the event when observation points start to record it and the value of the downdraft diameters.

CFD simulations

The Computational Fluid Dynamics (CFD) software, ANSYS CFX 14.0 (ANSYS CFX Reference Guide, 2011) has been used for simulating downburst flow as incompressible flow. The approved impinging wall jets models from several studies representing the transit dynamic properties and flow structure of downburst wind speed have been employed for the present study (Mason *et al*. 2005, Kim and Hangan 2007). The numerical simulation has been conducted twenty one times for different cases of intensity and decay periods.

The time step dt has been assumed to equal $(1/3600)\Delta t$, thus it generates approximately 3600 time steps during the total simulation period. Where Δt is the total simulation time, which equals the summation of Δt_I and Δt_d, Δt_I is the period of impinging flow with maximum speed and Δt_d is the rest of time after Δt_I during reducing or ceasing the inlet velocity until the end of the simulation. The driving mechanism for the downburst is given by the inlet jet velocity (V_{jet}) which equals 5 m/s for the period of time Δt_I, after which the inlet speed follows the decay functions during the period Δt_d.

The observed data of Wilson et al (1984) was employed for initial trials. Seven different values for Δt_I were used starting from Δt_I = 3 minutes, increasing by one minute intervals until Δt_I = 9 minutes while Δt is kept constant at 18 minutes. The corresponding values for Δt_d =$(\Delta t - \Delta t_I)$ are from 15 minutes

with decreasing intervals of 1 to 9 minutes respectively, for the field size model. These seven cases were repeated for three different cases of the inlet speed during the decay period Δt_d. The different decay functions for inlet velocity are given by Equations (1), (2) and (3).

$$V_{jet} = 0.0 \quad (1)$$

$$V_{jet} = \begin{cases} V_{jet}\, x\, cos^2\left[\pi\left(\frac{t-\Delta t_I}{\zeta t}\right)\right] & \Delta t_I \le t < (\Delta t_I + 1.5\ min) \\ \simeq 0.0 & t \ge (\Delta t_I + 1.5\ min) \end{cases} \quad (2)$$

$$V_{jet} = \begin{cases} V_{jet}\, x\, cos^2\left[\pi\left(\frac{t-\Delta t_I}{\zeta t}\right)\right] & \Delta t_I \le t < (\Delta t_I + 3\ min) \\ \simeq 0.0 & t \ge (\Delta t_I + 3\ min) \end{cases} \quad (3)$$

The previous periods are for the field size model and the corresponding periods for the numerical model are determined by scaling the time periods using the Shehata et al (2005) procedure.

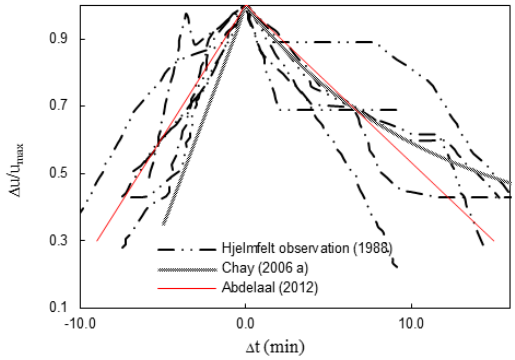

Figure 1. Normalised radial velocity versus time of downbursts.

Parametric study

A parametric study has been established and combined with the numerical results. The purpose of the parametric study is the creation of wide ranges for different parameters similar to field factors that have effect on events during field observation. Then, the coupled parametric-CFD study has been applied for several recorded field events to get the best appropriate field information.

The numerical results from CFD simulation had to undergo several adjustments to be comparable with the recorded field data. Firstly, the CFD results must be scaled to the observed wide range of downburst diameters, the utilized D_{jet} in the numerical model is 0.750 m whereas the observed range of downburst diameters in the field are 400 to 4000 m (Fujita 1981). The inlet jet speed also needed to be scaled to match the field range. Secondly, the transfer speed of the parent storm must be defined and added to the downburst speed. The direction of downburst path and the initial location also needed to be determined. Finally, the intensity period Δt_I and different cases of decay functions have to be substituted with different values until the best results can be determined.

The list of the parameters that were investigated during the present study are (D_{jet}, V_{jet}, V_{tran}, X_{org} and Y_{org}, α, Δt_I and $C\Delta t_d$). Where: D_{jet} and V_{jet} is the diameter and the inlet speed, V_{tran} is the parent storm translation speed, X_{org} and Y_{org} are the initial coordinates of the downburst event at $t = 0.0$, α is the angle between the direction of downburst path and X-axis direction (Figure 2), Δt_I is the intensity period and $C\Delta t_d$ is the approved equation for decaying the inlet jet speed from Equations (1), (2) and (3).

Parametric study procedure

Each of the parameters (D_{jet}, V_{jet}, V_{tran}, X_{org} and Y_{org}, α, Δt_I and $C\Delta t_d$) are independent variables and the object of the study is estimating the appropriate value for Δt_I and the other parameters as well. The best solution for these parameters will be the one that gives the smallest summation of the errors ($\sum_{t=0}^{t=T} F_t$) whilst matching the recorded data. T is the total time from start of impinging wind at cloud base till the end of the final decay of the event, and (F_t) is the summation of the two square errors as follows:

$$F_t = (fv_t)^2 + \Pi\,(f\theta_t)^2 \quad (4)$$

Where:

fv_t is the difference between the observed wind speed (vb_t) at time t and the wind speed (v_t) at a corresponding time t computed by the coupled parametric-CFD study and given by Equation (5).

$f\theta_t$ is the difference between the observed direction of wind speed (Θb_t) at time t and the direction of wind speed (Θ_t) at a corresponding time t computed by the coupled parametric-CFD study and given by Equation (6):

And Π is a scaling factor, used for scaling the wind direction error to be combinable with wind speed error, which has been selected to be = 0.1 $\left(\frac{m}{s}/deg\right)$.

$$fv_t = [v_t\,(D_{jet}, V_{jet}, V_{tran}, X_{org}, Y_{org}, \alpha, \Delta t_I, C\Delta t_d) - vb_t] \quad (5)$$

$$f\theta_t = [\Theta_t(D_{jet}, V_{jet}, V_{tran}, X_{org}, Y_{org}, \alpha, \Delta t_I, C\Delta t_d) - \Theta b_t] \quad (6)$$

Then the following steps have been done for estimating the appreciated Δt_I and the other parameters for each inspected event:

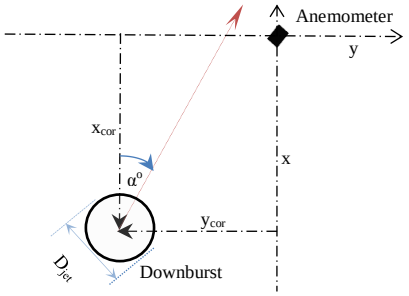

Figure 2. Horizontal projection of the downburst and the anemometer.

- For each case from the 21 numerical simulation cases for small model ($D_{jet} = 0.75$ m, $V_{jet} = 5.0$ m/s) the distribution of wind speed on any line that extended from centre of the model to the outlet end of the model is assumed to be representative of downburst wind speed. The horizontal speeds on such lines have been collected at a time step = 0.0162 s during the total simulation periods (from $t = 0.0$ s until $t = 6.48$ s) and at height $Z = 0.015D_{jet}$.

- The different parameters are described according to the observed field data. The downburst diameter D_{jet} has been applied in the range from $D_{jet} = 400$ m until $D_{jet} = 4000$ m with an increasing step equal $0.02D_{jet}$. The initial location of the downburst at time t= 0 is unknown so that ranges are suggested for X_{org} and Y_{org}. The inlet jet field speed (V_{jet}) is assumed to produce peak horizontal speed in the range (1.0 up to 1.3 m/s) of maximum recorded speed with increasing step 0.05 m/s from maximum recorded field speed.

- The observed transfer speed may differ from the actual speed due to the effect of the mesoscale pressure gradient that results from previous convective activity (Holmes et al 2008). Hence the translation speed has been given in a range of ≃ ± 2.5 m/s from the observed value before passing the event and added by step 0.2 m/s.

- The following Pseudo-code has been run for matching both the recorded wind speed and the wind direction, computing

the error functions $\left(\sum_{t=0}^{t=T} F_t\right)$ and estimating the appreciated Δt_I and the other parameters for every inspected event. The code runs through the following steps:

- Several loops have been prepared for all the parameters through the suggested ranges and increasing steps.
- The parameters are elected according to the loop number.
- The CFD results (21 files) are scaled to the elected D_{jet}, V_{jet}.
- Inside each loop the following calculations run for 400 time steps ($\delta t = T/400$) during the total period T.

i. At t=0, the downburst wind speed $\vec{V}_{burst} = 0.0$ then $\vec{V}_t = \vec{V}_{tran}$ and $\Theta_t = \alpha$.
ii. At the next time step $t = \delta t$, the storm travels a distance $L = V_{tran} \times t$ according to the suggested path, then the two components for the change in the location of downburst (ΔX_{cor} and ΔY_{cor}) are computed and the new location is determined.
iii. From the stored numerical files, the downburst horizontal wind speed $\vec{V}_{burst}$ at a distance equal to the distance between the downburst and observation point is obtained.
iv. The sum of the two wind speeds $\vec{V}_t = \vec{V}_{tran} + \vec{V}_{burst}$ and wind direction $\Theta_t = \tan^{-1}(\vec{V}_t x / \vec{V}_{ty})$ are calculated.
v. The same procedure is repeated at every time step until $t = T$.
vi. After finishing the loop, the error function is computed $\sum_{t=0}^{t=T} F_t$ and stored.

- Repeat the previous steps for new parameters and at the end of each loop the error function is calculated and stored.
- After finishing all the loops, all the error functions are compared and the parameters that correspond to the minimum error function are evaluated.

- The Pseudo-code is repeated for each studied event.

The utilised field data

Several events have been used for estimating the ages of downbursts and for improving the study results. The first employed event was recorded at Andrews Air Force Base (AAFB), near Washington, D.C., U.S.A in 1983 (Fujita 1985). The second event occurred in the Rondonia region of the Brazilian Amazon on 17 February 1999 (Atlas et al 2004). The next pair of events took place near Brisbane Airport at around 2129 UTC, 17 January 2001(FSF 2003) and the full-scale rear-front downburst recorded from tower 4 at Reese Air Force Base (RAFB), near Lubbock, Texas, U.S.A in 2002 (Gast and Schroeder, 2005). The last event occurred in Hyytiälä (Juupajoki, Finland) on the afternoon of 3 July 2004 (Järvi et al 2007).

Results and discussion

The present study depicted with high accuracy the different recorded profiles for the investigated events (Figure 3 to Figure 7). Although the results of the current study have been estimated by comparing the least square errors, the presented techniques could be developed to a mathematical procedure since they depend on logical relationships. For example, the profile of wind direction provides some information about the original location and path direction of the event. When the magnitude of wind speed increases without a change in wind direction, it means that the event was born far from the observation point and is approaching the observation point but did not cross it yet (e.g. the first 300 secs in Figure 3). While in the case of changing wind direction during the first observations, it means that the event was born very close to the observation point (Figure 7). In addition, the rate of change in the wind direction gives information about the direction of downburst path. If the change is sharp (Figure 6) that means the events pass perpendicular to the observation points, while the slow change means that the events move with deviation about the observation points. The rate of change in magnitude of wind speed during intensity and decay can provide information about the relationship between the transverse orientation and α. The wind speed profile contributes to determining the remainder of the parameters as well.

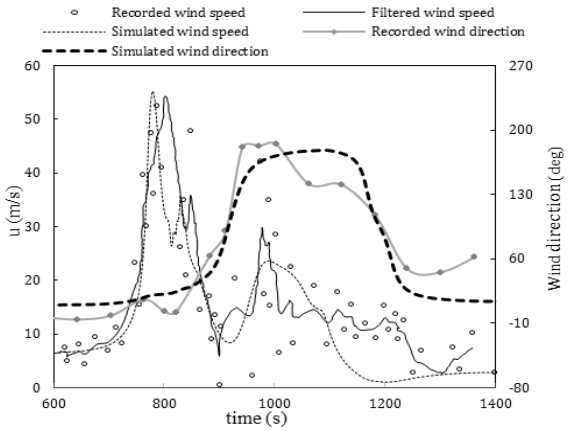

Figure 3. Recorded and simulated wind speed and wind direction at Andrews AFB downburst.

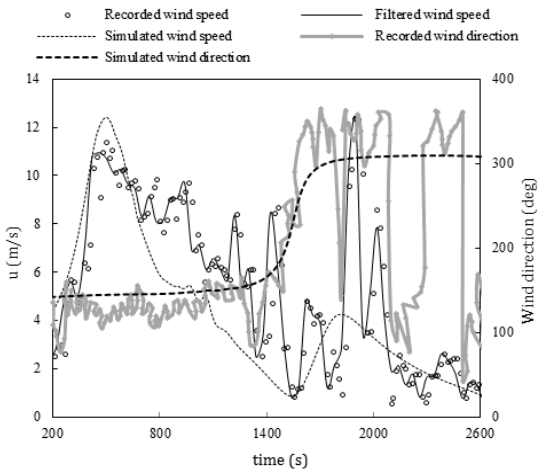

Figure 4. Recorded and simulated wind speed and wind direction at Rondonia region.

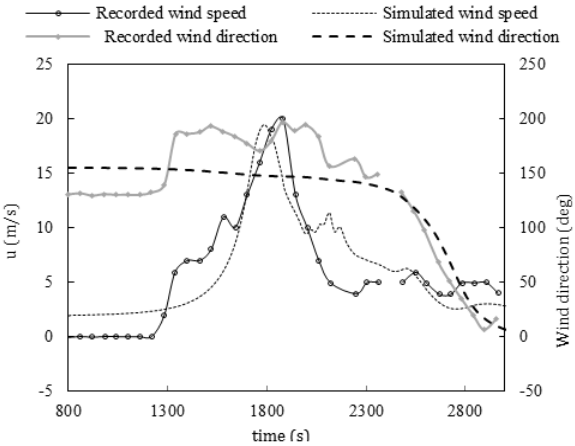

Figure 5. Recorded and simulated wind speed and wind direction at Brisbane Airport.

The estimated parameters for each of the examined events are collected in Table 1. The given values for Δt_I and $C\Delta t_d$ in Table

1 are for the equivalent model ($D_{jet} = 750$ m, Jet height =3.5 D_{jet} and V_{jet}= 30 m/s) before scaling it for the actual field scale. The studied events showed the value of Δt_I to be in the range of 4 to 7 minutes for the model ($D_{jet} = 750$ m, Jet height =3.5 D_{jet} and V_{jet}= 30 m/s).

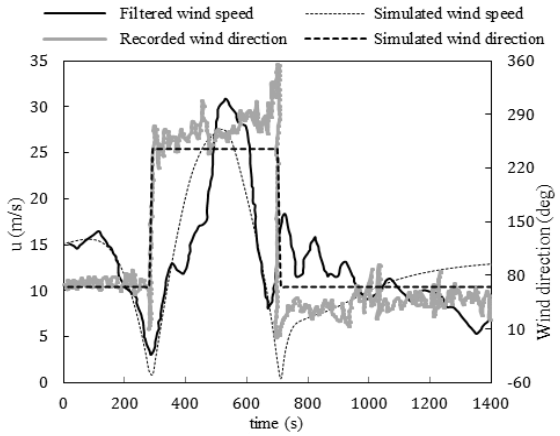

Figure 6. Recorded and simulated wind speed and wind direction at Reese Air Force Base.

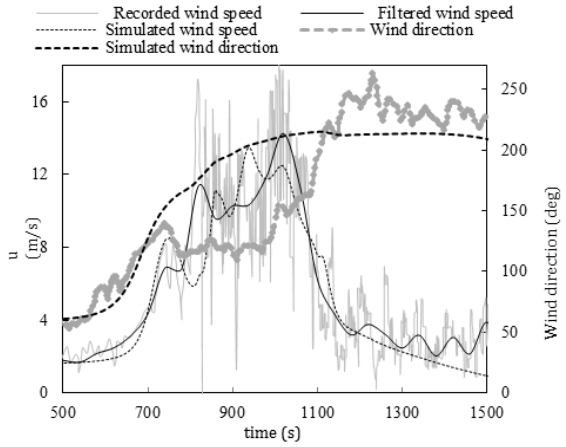

Figure 7. Recorded and simulated wind speed and wind direction at Hyytiälä.

The event	D_{jet} (m)	V_{tran} (m/s)	X_{cor} (m)	Y_{cor} (m)	α $(deg.)$	Δt_I (min)	Δt_d (min)
AFB	660	6.5	-490	-490	10	7	1.5
Rondonia	1750	1.85	-400	-400	7	4	0
Brisbane	1775	1.9	-70	-70	5	4	0
RAFB	2850	13.5	-9100	0	0	-------	--------
Hyytiälä	510	1.6	-400	-400	35	5	3

Table 1. The estimated parameters for the studied events

Conclusion

This parametric-CFD study presented the following points:

- A new technique for researching the downburst events has been established. The new technique is distinguished by the ability to estimate the different downburst parameters through the observed magnitude and direction of wind speed.
- A new approach for measuring the ages of downbursts has been developed to avoid the effects of different field parameters, by measuring the period of impinging flow from jet inlet instead of the recorded periods that are too sensitive to different field parameters. The ages of various investigated downbursts are in the range of 4 to 7 minutes, when compared to equivalent downburst ($D_{jet} = 750$ m, Jet height =3.5 D_{jet} and V_{jet}= 30 m/s).

REFERENCES

Abd-Elaal E, Mills J, Ma X (2012) A newly developed analytical model of transient downburst wind loads. Proceedings of the 22nd Australian Conference on the Mechanics of Structures and Materials, Sydney, Australia, pp 425 - 430.

Anderson R, Orf G, Straka M (1992) A 3-D model system for simulating thunderstorm microburst outflows, Meteorology and Atmospheric Physics 49:125–131.

ANSYS CFX Reference Guide (2011) Release 14.0, ANSYS, Inc. November 2011.

Atlas D, Ulbrich W, Williams R (2004) Physical Origin of a Wet Microburst: Observations and Theory, Journal of the Atmospheric Sciences 61:1186-1196.

Bureau of Meteorology (2013) Storm archive data. <http://www.bom.gov.au/australia/stormarchive/ 2013> (accessed February 2013).

Chay T, Albermani F, Wilson R (2006) Numerical and analytical simulation of downburst wind loads, Engineering Structures 28(2):240-254.

FSF Editorial Staff (2003) Inadequate Weather Communication Cited in B-737 Microburst-downdraft incident, Airport Operations 29(1).

Fujita T (1981) Tornadoes and Downbursts in the Context of Generalized Planetary Scales, Journal of the Atmospheric Sciences 38 (8): 1511-1534.

Fujita T (1985) The downburst Report of Projects NIMROD and JAWS. The University of Chicago.

Gast D, Schroeder L (2005) Extreme wind events observed in the 2002 thunderstorm outflow experiment. In: Proceedings of the 10th Americas Conference on Wind Engineering (10 ACWE), Baton Rouge, LA, USA.

Hjelmfelt R (1988) Structure and Life Cycle of Microburst Outflows Observed in Colorado, Journal of Applied Meteorology 27(8): 900-927.

Holmes D, Hangan M, Schroeder L, Letchford W, Orwig D (2008) A forensic study of the Lubbock-Reese downdraft of 2002, Wind and structures 11(2): 137-152.

Järvi L, Punkka J, Schultz M, Petäjä T, Hohti H, Rinne J, Pohja T, Kulmala M, Hari P, Vesala T (2007) Micrometeorological observations of a microburst in southern Finland, Boundary-Layer Meteorology 125:343-359.

Kim J, Hangan (2007) Numerical simulations of impinging jets with application to downbursts, Journal of Wind Engineering and Industrial Aerodynamics 95(4): 279-298.

Mason S, Letchford W, James L (2005) Pulsed wall jet simulation of a stationary thunderstorm downburst, Part A: Physical structure and flow field characterization, Journal of Wind Engineering and Industrial Aerodynamics 93(7): 557-580.

ShehataY, El Damatty A, Savory E (2005) Finite element modeling of transmission line under downburst wind loading, Finite Elements in Analysis and Design 42(1): 71-89.

Wilson W, Roberts D, Kessinger C, McCarthy J (1984) Microburst wind structure and evaluation of Doppler radar for airport wind shear detection, Journal of Climate and Applied Meteorology 23(6):898–915.